ELSEVIER

Journal of Organometallic Chemistry 524 (1996) 9–18

Journal of Organometallic Chemistry

Molecular structure of α,α-carbonium [1.1]ferrocenylruthenocenophane + BF_4^- salt

Masanobu Watanabe *, Izumi Motoyama, Toshio Takayama

Department of Chemistry, Faculty of Engineering, Kanagawa University, Rokkakubashi, Yokohama 221, Japan

Received 15 November 1995; in revised form 10 January 1996

Abstract

The oxidation of [1.1]ferrocenylruthenocenophane (**1**) with bromo- or chlororuthenocenium $^+BF_4^-$ ([RcHX]$^+BF_4^-$; X = Br, Cl) was carried out giving a diamagnetic salt **2**. The crystal form of **2** is monoclinic, space group $P2_1/n$, $a = 10.556(3)$, $b = 13.634(3)$, $c = 13.795(2)$ Å, $\beta = 107.27(2)°$, $V = 1896.0(8)$ Å^3, $Z = 4$, and the final $R = 0.045$ and $R_w = 0.040$, based on the results of the single-crystal X-ray diffraction study. The distance between the Ru and Fe is ca. 4.495(2) Å, which is much shorter than **1** (4.792(2) Å). The structure of the cation is illustrated as a resonance hybrid canonical structure of α,α-carbonium-type expressed as $[Fe^{II}(C_5H_4CH_2C_5H_4)(C_5H_4CHC_5H_4)Ru]^+$ and η^6-fulvalne-type as $[Fe^{II}(C_5H_4CH_2C_5H_4)(C_5H_4CH{=}C_5H_4)Ru]^+$. The two C_5H_4 rings on the Ru side are tilted greatly (the dihedral angle of the rings is 10.92°) owing to the Ru–C_α^+ bond formation (2.407(6) Å), which gives the stability of the carbonium center –CH^+–. ^{57}Fe Mössbauer, ^{1}H, ^{13}C and ^{13}C CP/MAS NMR spectroscopic studies support the above formula.

Keywords: Iron; Ruthenium; Ferrocene; Metallocenes

1. Introduction

Recently, we have reported the structure of the oxidation product of **1** with iodoruthenocenium $^+BF_4^-$ ([RcHI]$^+BF_4^-$), which is formulated as $[Fe^{II}(C_5H_4CH_2C_5H_4)_2Ru^{IV}I]^+BF_4^-$ with a stable Ru^{IV}–I bond (2.751(1) Å) on the basis of the results of X-ray diffraction and ^{13}C CP/MAS NMR spectroscopy [1]. Therefore, it is clear that the formation of the Ru^{IV}–I bond occurs predominantly over the formation of ferrocenium salt formulated as $[Fe^{III}(C_5H_4CH_2C_5H_4)_2Ru^{II}]^+BF_4^-$, while the Fe is oxidized more easily than the Ru atom in **1** on the basis of the result of cyclic voltammograms [2]. In the present study, oxidation of **1** with other haloruthenocenium salts, such as [RcHBr]$^+BF_4^-$ or [RcHCl]$^+BF_4^-$, are reported. The oxidation product was not an oxidized metallocene; it was neither a typical paramagnetic ferrocenium salt $[Fe^{III}(C_5H_4CH_2C_5H_4)_2Ru^{II}]^+BF_4^-$ nor a diamagnetic haloruthenocenium salt $[Fe^{II}(C_5H_4CH_2C_5H_4)_2Ru^{IV}X]^+BF_4^-$ (X = Cl, Br), but an α,α-carbonium salt **2**. (Scheme 1) The crystallographic analysis and ^{57}Fe, ^{1}H, ^{13}C and ^{13}C CP/MAS NMR spectroscopic studies of **2** will be discussed and compared with those of **1** and **3** in this paper.

2. Experimental

2.1. Syntheses

Salt **2** was prepared as follows: the neutral compound **1** (100 mg, 0.227 mmol; prepared by the reduction of [1.1]ferrocenylruthenocene-1,13-dione with $LiAlH_4$ and $AlCl_3$ by the method reported previously [3]) dissolved in 50 cm^3 of CH_2Cl_2 was added to a stoichiometric amount of [RcHBr]$^+BF_4^-$ or [RcHCl]$^+BF_4^-$ dissolved in 200 cm^3 of CH_2Cl_2. The mixture was stirred for 1 h and the solvent was evaporated. After extraction of RcH with benzene, **2** was obtained by recrystallization from a CH_3CN–$C_2H_5OC_2H_5$ mixture as dark purple crystals (95 mg; yield 79%). Single crystals suitable for X-ray studies were obtained by diffusion of ether vapor into CH_3CN solution of **2** at room temperature. Found:

* Corresponding author.

PII S0022-328X(96)06156-6

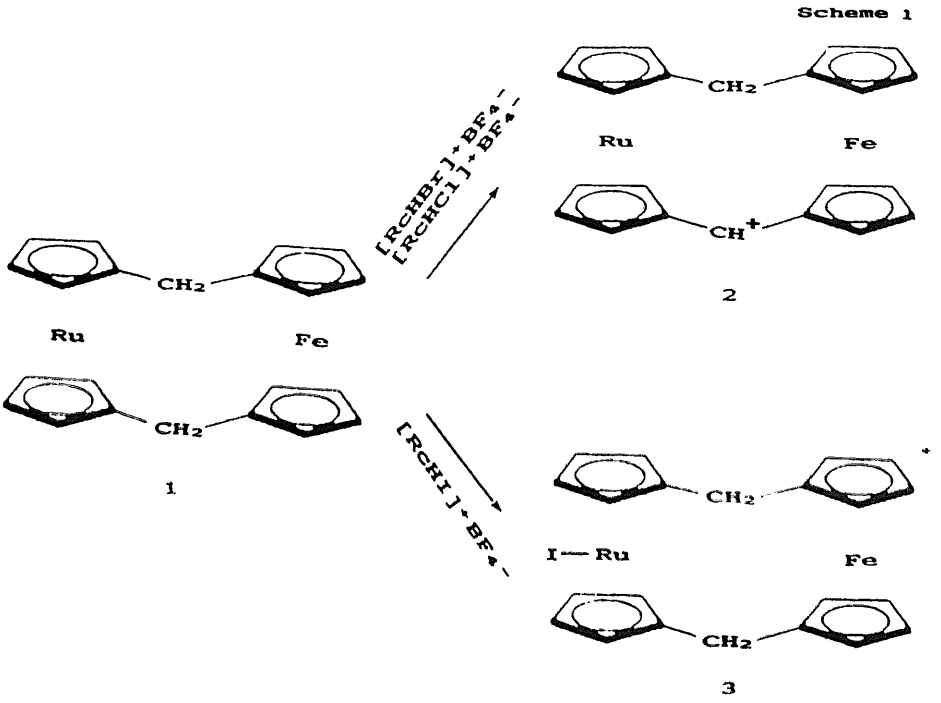

Scheme 1.

C, 50.09; H, 3.59. $C_{22}H_{19}BF_4FeRu$. Calc.: C, 50.13; H, 3.63%.

2.2. Measurements

2.2.1. NMR spectroscopy

^1H (500.16 MHz) and ^{13}C (125.65 MHz) NMR spectra were recorded on a Jeol Alpha 500 spectrometer fitting with a multinuclear probe in acetonitrile-d_3 and acetone-d_6 as the sample solvent. The ^1H and ^{13}C NMR chemical shifts were calibrated indirectly through the internal CH_3CN ^1H signal (1.96 ppm relative to TMS) and acetone-d_6 ^{13}C signal (30.4 ppm relative to TMS). Peak assignments were carried out by using DEPT, NOESY and COSY [4] spectra. All measurements were carried out at 25.0 ± 0.1°C. ^{13}C CP/MAS NMR spectra were recorded on a Jeol EX-270 NMR spectrometer operating at 67.8 MHz with a CP/MAS accessory under the similar conditions to those reported previously [1]. The ^{13}C NMR chemical shifts were calibrated indirectly through external adamantane (29.5 ppm relative to TMS). The experimental error in the ^{13}C chemical shifts is estimated to be about 0.1 ppm. The dipolar dephasing (DD) experiment is a method for obtaining the analogous nonprotonated carbon spectrum for solid samples. In the DD experiment, the ^{13}C DD time was determined by measuring the ^{13}C CP/MAS NMR spectra, varying the delay time τ for the proton dipolar decoupling and data acquisition in the range of 10–60 μs (20 μs in this experiment), which was long enough to eliminate the ^{13}C signals of all protonated carbons). It must be pointed out that under these conditions the relative peak intensities measured with CP/MAS and DD/MAS are not a true measure of the abundances of the carbon atoms because not every carbon atom has attained its optimum cross-polarization and its optimum delay time. ^{57}Fe Mössbauer measurements were carried out using a $^{57}Co(Rh)$ source moving in constant acceleration mode. The isomer shift (IS) value was referred to metallic iron foil. The Mössbauer parameters were obtained by least squares fitting to Lorentzian peaks. The experimental error of the IS and quadrupole splitting (QS) values was 0.02 mm s^{-1}.

2.2.2. X-ray crystallography

Crystals of **1** (0.2 × 0.2 × 0.3 mm^3) were selected. X-ray diffraction experiments were carried out on a Rigaku AFC-6A automated four-circle X-ray diffractometer with graphite monochromatized Mo Kα radiation (λ = 0.71073 Å). The intensity data were collected at 25 ± 1° using the ω–2θ scan mode with a scanning speed of 4° min^{-1}. The lattice parameters were determined by a least squares calculation with 25 reflections. Crystal stability was checked by recording three standard reflections every 150 reflections, and no significant variations were observed. For **1**, 6038 reflections were collected in the range $4 \leq 2\theta \leq 60°$, 5760 were unique (R_{int} = 0.019), of which 3455 reflections with $I_{obsd} > 1.5\sigma$ (I_{obsd}) were used for the structure determination. The scan width was 1.78 + 0.3 tan θ. The refinement

Table 1
Crystal and intensity collection data for 2

Formula	$C_{22}H_{19}BF_4FeRu$
Formula weight	527.11
Space group	$P2_1/n$
a (Å)	10.556(3)
b (Å)	13.634(3)
c (Å)	13.795(2)
β (deg)	107.27(2)
V (Å^3)	1896.0(8)
Z	4
D_x (g cm^{-3})	1.846
T (°C)	25
λ (Å)	0.71073
μ (cm^{-1})	16.04
$F(000)$	1048
No. of radiations measured	6038
No. of observed	3455 ($I > 1.5\sigma(I)$)
R	0.045
R_w	0.040

262 variable parameters converged to $R = \Sigma \| F_0 \| - | F_c \| / \Sigma | F_0 | = 0.045$, $R_w = [\Sigma w(| F_0 | - | F_c |)^2 / \Sigma w F_0^2)]^{1/2} = 0.040$, and the standard deviation of an observation of unit weight was 2.26.

The nonhydrogen atoms were refined anisotropically by full matrix least squares. Hydrogen atoms were located based on difference Fourier maps, and were included isotropically in the refinement. Neutral atom scattering factors were taken from Cromer and Waber [5]; anomalous dispersion effects corrections were included in F cal [6], the values for $\Delta f'$ and $\Delta f''$ were those of Creagh and McAuley [7]. All of the calculations were performed using the TEXSAN crystallographic software package [8]. Crystallographic data and some of the experimental conditions for the X-ray structure analysis are listed in Table 1.

3. Results and discussion

The final atomic coordinates and equivalent isotropic temperature factors B_{eq} of nonhydrogen atoms, selected bond distances, and angles for **2** are shown in Tables 2–5 and ORTEP drawings of the cations **2** system are shown in Fig. 1 with the atom numbering. The cation remains in syn-conformation as with **1** and **3**. In contrast with **3**, no bond formation between the Ru and X (X = Cl, Br) was observed. The distance between the Fe(1) and Ru(1) is 4.495(2) Å, suggesting no interaction between them, although the value is much smaller than the corresponding values of **1** (4.792(2) Å [9]) and **3** (4.719(1) Å) [1], see Table 6. The Fe–C_{ring} and Fe–Cp distances are 2.04(1) Å and 1.643(4) Å respectively, which are comparable with the equivalent values of **1** (2.055(6) and 1.665(7) Å) and FcH (2.045 and 1.65 Å [10]); i.e. the oxidation state of the Fe in **2** remains intact.

The most interesting structural feature of **2** is found in the distance of C(22)–Ru(1) (2.407(6) Å), which is much shorter than the corresponding values in **1** and **3**, although the distances between the C(22) · · · Fe(1) (3.155(5)), C(21) · · · Fe(1) (3.207(7)) and C(21) · · · Ru(1) (3.405(6) Å) are comparable with those of **3** (Fe(1) · · · C(21) (3.246(7)), Fe(1) · · · C(22) (3.208(6)), Ru(1) · · · C(21) (3.417(7)) and Ru(1) · · · C(22) (3.450(7) Å) [1]. However, the Ru(1)–C(22) distance is ca. 0.15 Å smaller than the sum of the covalent radii of C (0.77 Å [11]) and Ru (1.49 Å [12]), which is considered to be strong evidence of bond formation between the Ru and carbonium center C(22) atoms. Furthermore, it is clear that the the C(21) and C(22) are methylene and methine in character respectively, on the results of difference Fourier maps (all the H atoms are located based on the maps). Therefore, the cation **2** is formulated as $[Fe(C_5H_4CH_2C_5H_4)(C_5H_4CH^+C_5H_4)Ru]$ with an Ru–CH^+ bond. This conclusion is confirmed by the results of ^{57}Fe Mössbauer spectroscopy of **1**; i.e. only the ferrocene-like doublet line was observed. The QS and IS values are found to

Table 2
Atomic coordinates and B_{iso} / B_{eq} for 2

Atom	x	y	z	B_{eq}
Ru(1)	0.05481(5)	0.13605(3)	−0.22235(3)	2.671(9)
Fe(1)	−0.33641(8)	0.19938(6)	−0.16790(6)	2.84(2)
F(1)	0.6151(5)	0.1031(3)	0.4368(3)	7.8(1)
F(2)	0.6144(5)	0.0223(4)	0.2971(4)	9.7(2)
F(3)	0.7936(5)	0.0952(4)	0.3864(4)	9.1(2)
F(4)	0.7239(5)	−0.0367(3)	0.4475(4)	9.7(2)
C(1)	−0.3018(6)	0.2922(4)	−0.2737(4)	3.7(1)
C(2)	−0.3997(6)	0.2226(5)	−0.3225(4)	4.5(2)
C(3)	−0.5065(6)	0.2300(6)	−0.2808(5)	5.8(2)
C(4)	−0.4767(8)	0.3054(6)	−0.2069(6)	6.3(2)
C(5)	−0.3508(8)	0.3443(5)	−0.2025(5)	5.4(2)
C(6)	−0.1579(5)	0.1456(4)	−0.0823(3)	2.7(1)
C(7)	−0.2400(5)	0.0680(4)	−0.1365(4)	2.7(1)
C(8)	−0.3582(5)	0.0657(4)	−0.1086(4)	3.1(1)
C(9)	−0.3501(5)	0.1416(5)	−0.0361(4)	3.6(1)
C(10)	−0.2289(6)	0.1909(4)	−0.0213(4)	3.3(1)
C(11)	−0.0919(5)	0.2394(4)	−0.3211(4)	3.0(1)
C(12)	−0.1239(5)	0.1399(4)	−0.3534(4)	3.1(1)
C(13)	−0.0168(7)	0.1013(5)	−0.3820(4)	4.1(2)
C(14)	0.0826(6)	0.1733(5)	−0.3671(4)	4.2(2)
C(15)	0.0368(6)	0.2580(5)	−0.3288(4)	3.8(1)
C(16)	0.0843(5)	0.1158(4)	−0.0678(4)	3.1(1)
C(17)	0.0700(5)	0.0179(4)	−0.1133(4)	3.1(1)
C(18)	0.1764(6)	0.0057(4)	−0.1543(4)	3.8(1)
C(19)	0.2581(6)	0.0914(5)	−0.1329(5)	4.2(2)
C(20)	0.2053(5)	0.1583(4)	−0.0787(4)	3.7(1)
C(21)	−0.1755(6)	0.3177(4)	−0.2943(4)	3.8(1)
C(22)	−0.0255(5)	0.1777(4)	−0.0815(4)	2.8(1)
B(1)	0.6837(8)	0.0447(6)	0.3898(7)	4.7(2)
H(22)	−0.004(4)	−0.254(3)	0.434(3)	1.6(1)

Table 3
Intramolecular distances for 2

Atom	Distance (Å)	Atom	Distance (Å)
Fe(1)–Ru(1)	4.495(2)	Fe(1)–C(1)	2.044(6)
Fe(1)–C(2)	2.061(6)	Fe(1)–C(3)	2.041(6)
Fe(1)–C(4)	2.025(8)	Fe(1)–C(5)	2.027(6)
Fe(1)–C(6)	2.040(5)	Fe(1)–C(7)	2.043(5)
Fe(1)–C(8)	2.039(6)	Fe(1)–C(9)	2.026(6)
Fe(1)–C(10)	2.008(5)	Fe(1)–C(21)	3.207(7)
Fe(1)–C(22)	3.155(5)	Ru(1)–C(11)	2.234(5)
Ru(1)–C(12)	2.192(5)	Ru(1)–C(13)	2.159(5)
Ru(1)–C(14)	2.163(7)	Ru(1)–C(15)	2.189(6)
Ru(1)–C(16)	2.079(5)	Ru(1)–C(17)	2.177(6)
Ru(1)–C(18)	2.230(6)	Ru(1)–C(19)	2.219(5)
Ru(1)–C(20)	2.162(5)	Ru(1)–C(21)	3.405(6)
Ru(1)–C(22)	2.407(6)	C(1)–C(2)	1.42(1)
C(2)–C(3)	1.41(1)	C(3)–C(4)	1.42(1)
C(4)–C(5)	1.42(1)	C(5)–C(1)	1.43(1)
C(6)–C(7)	1.43(1)	C(7)–C(8)	1.41(1)
C(8)–C(9)	1.42(1)	C(9)–C(10)	1.41(1)
C(10)–C(6)	1.42(1)	C(1)–C(21)	1.49(1)
C(11)–C(21)	1.50(1)	C(11)–C(12)	1.44(1)
C(12)–C(13)	1.41(1)	C(13)–C(14)	1.41(1)
C(14)–C(15)	1.41(1)	C(15)–C(11)	1.42(1)
C(16)–C(17)	1.46(1)	C(17)–C(18)	1.41(1)
C(18)–C(19)	1.43(1)	C(19)–C(20)	1.40(1)
C(20)–C(16)	1.45(1)	C(6)–C(22)	1.46(1)
C(16)–C(22)	1.40(1)	B(1)–F(1)	1.363(9)
B(1)–F(2)	1.308(9)	B(1)–F(3)	1.362(9)
B(1)–F(4)	1.357(9)	H(21a)–C(21)	0.94(4)
H(21b)–C(21)	0.95(4)	H(22)–C(22)	0.97(4)
H(22)–F(1)	2.40(4)		

Table 4
Bond angles (deg) for 2

C(1)–C(2)–C(3)	108.4(6)	C(2)–C(3)–C(4)	108.1(7)
C(3)–C(4)–C(5)	107.9(8)	C(4)–C(5)–C(1)	108.2(6)
C(5)–C(1)–C(2)	107.3(6)	C(6)–C(7)–C(8)	108.7(5)
C(7)–C(8)–C(9)	107.6(5)	C(8)–C(9)–C(10)	108.2(5)
C(9)–C(10)–C(6)	108.9(5)	C(7)–C(6)–C(10)	106.6(5)
C(5)–C(1)–C(21)	123.0(5)	C(2)–C(1)–C(21)	129.4(6)
C(10)–C(6)–C(22)	122.4(4)	C(7)–C(6)–C(22)	130.9(5)
C(15)–C(11)–C(12)	106.7(5)	C(11)–C(12)–C(13)	107.9(5)
C(12)–C(13)–C(14)	108.9(6)	C(13)–C(14)–C(15)	107.6(6)
C(14)–C(15)–C(11)	108.9(5)	C(12)–C(11)–C(21)	130.3(5)
C(15)–C(11)–C(21)	122.7(5)	C(17)–C(16)–C(22)	121.0(4)
C(20)–C(16)–C(22)	117.7(5)	C(1)–C(21)–C(11)	120.6(5)
C(6)–C(22)–C(16)	124.9(5)	Ru(1)–C(22)–C(16)	59.4(3)
Ru(1)–C(22)–C(6)	119.2(3)	H(22)–C(22)–C(16)	113.9(3)
H(22)–C(22)–C(6)	116.8(4)	F(1)–B–F(2)	112.3(7)
F(1)–B–F(3)	107.4(7)	F(1)–B–F(4)	108.5(8)
F(2)–B–F(3)	108.6(8)	F(2)–B–F(4)	111.7(7)
F(3)–B–F(4)	108.2(6)		

Table 5
Dihedral angle between the planes (deg) for 2

	Plane		
	C(6–10)	C(11–15)	C(16–20)
C(1–5)	3.46	24.93	18.55
C(6–10)		21.47	15.51
C(11–15)			10.92

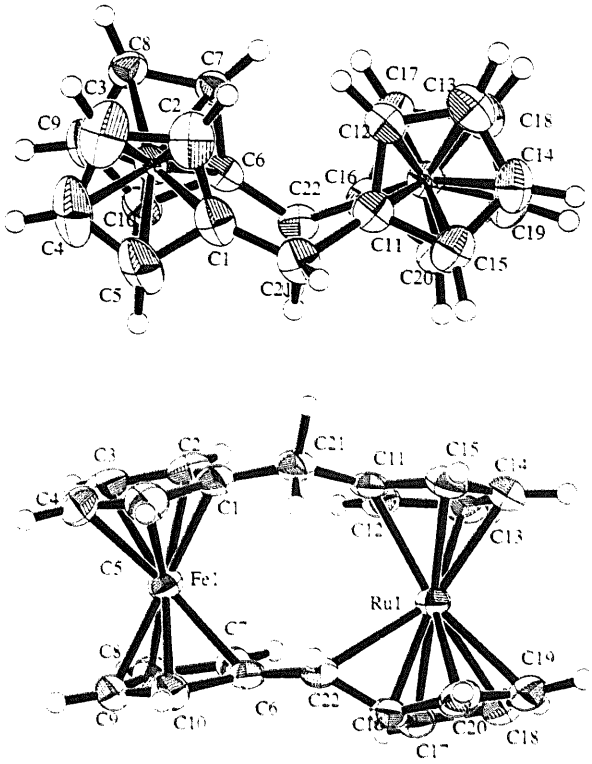

Fig. 1. ORTEP drawing of cation 2 with thermal ellipsoids at the 50% probability level. Perspective view with atomic numbering scheme (bottom) and projection of a whole molecule onto the Cp plane (top).

be 1.89, 0.50 mm s^{-1} at 78 K and 1.86, 0.42 mm s^{-1} at 300 K. The much smaller QS values of 2 compared with the value of 1 (2.41 at 78 K and 2.40 mm s^{-1} at 300 K) must be explained by the strong electron-attractive ($C_5H_4CH^+C_5H_4$) group.

The bond formation C(22)–Ru gives a large inclination angle ($\beta = 35.1°$) of the C(16)–C(22) bond to the plane C(16–20) ($\beta = 6.7°$ for exocyclic C(11)–C(21) bond to the η^5-C_5H_4 plane C(11–15)), as shown in Fig. 2. Nonplanarity of C_5H_4 plane C(16 ~ 20) is explained by the same reason; i.e. the bending angle α between the plane C(17 ~ 20) and the C(20)–C(16)–C(17) is ca.

Table 6
Selected bond lengths (Å) and angles (deg) of 2, 3 and 1

	2	3	1
Fe ··· Ru	4.495(2)	4.719(1)	4.792(2)
Fe–Cp	1.643(4)	1.654(2)	1.665(7)
Ru–Cp	1.801(4)	1.861(8)	1.788(5)
Ru–CH*	2.407(6)	–	–
Fe ··· CH*	3.208(6)	–	–
Fe–C_{rng}(av)	2.04(1)	2.047(6)	2.055(6)
Ru–C_{rng}(av)	2.18(4)	2.22(3)	2.151(6)
C_{rng}–C_{rng}(Fe)	1.42(1)	1.42(1)	
C_{rng}–C_{rng}(Ru)	1.42(3)	1.42(3)	
C(1)–C(21)–C(11)	120.6(5)	121.0(5)	120.4(5)
C(6)–C(22)–C(16)	124.9(5)	119.0(5)	120.7(5)

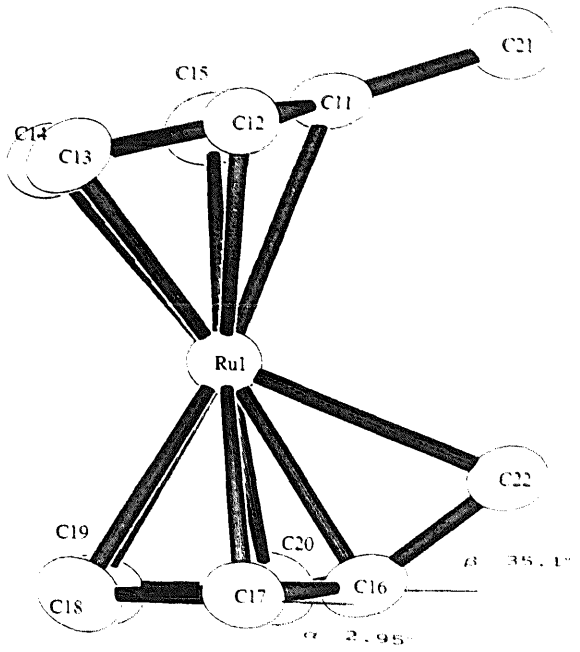

Fig. 2. ORTEP drawing of $CpC_5H_4RuCH^+$ moiety.

2.95°, while α between the planes C(12 ~ 15) and C(15)–C(11)–C(12) is ca. 1.27°. The much smaller Ru(1)–C(16) distance (2.079(5) Å) compared with other Ru(1)–C distances (2.159–2.234 Å), see Table 3, is due to the movement of C(16) and Ru(1) toward each other. Owing to this, and the steric hindrance between the C(11) and C(22) (the distance between the C(11) and C(22) (3.279(7) Å) is much smaller than the sum of van der Waals radii of two C (3.40 Å)), the two η^5-C_5H_4 rings of the Rc moiety are tilted greatly. The dihedral angle between them is 10.92°, while it is 3.46° for the Fc moiety.

The much smaller M–C^+ distances and larger β values compared with the values of **2** are reported in α-carbonium nonamethylruthenocenium and nonamethylosmocenium cations formulated as $[C_5(CH_3)_5C_4(CH_3)_4CH_2^+M]$ (M = Ru and Os, respectively); i.e. the covalent M–CH^+ bonds (2.270 Å and 2.244 Å respectively) and β (40.3° and 41.8° respectively) are found [13]. The shorter M–CH^+ bond and larger β value of the Os compound compared with those of analogous Ru are due to the stability of the Os–C^+ bond. For a long time, extensive discussions on the mechanism of stability of the α-carbonium in metallocene derivatives have been reported [13–17]. The stability of the α-carbonium $MCpC_5H_4CH_2^+$ ion is strongly dependent on the central metal atoms, i.e. the stability increases in the order Fe ≪ Ru < Os because of the increase in the atomic size (the covalent radii of Fe, Ru, Os are 1.34 Å, 1.49 Å, 1.50 Å respectively [12]), and its basicity. Therefore, the carbonium center –$C(22)^+$– in cation **2** is stabilized by the bond formation between the electronically softer Ru, which gives longer Ru–C_{ring} and Ru–Cp distances, i.e. the distances are 2.18(4) Å and 1.801(4) Å respectively; both values are larger than the corresponding values of **1** (2.151(6) Å, 1.788(5) Å respectively) with formal oxidation state Ru^{II}. Thus, the oxidation state of Ru in **2** has a more positive charge than Ru^{II} in neutral **1**.

The two η^5-C_5H_4 rings of each Fc and Rc moieties rotate ca. 9.7(6)° for Fc and 11.6(5)° for Rc moieties (the angle is ca. 13° for **1** [9]; 0° for perfectly eclipsed and 36° for staggered). The exocyclic distance C(16)–C(22) (1.40(1) Å) is significantly shorter than the other exocyclic C C bond lengths (1.46(1) Å for C(6)–C(22), 1.49(1) Å for C(1)–C(21) and 1.50(1) Å for C(11)–C(21)). The latter three bond lengths are comparable with the corresponding values of **3** (cf. 1.50(1) Å for C(1)–C(21) and 1.49(1) Å for C(11)–C(21)). The former value (1.40(1) Å) is closer to the intermediate values of single- (1.54 Å) and double-bond (1.33 Å) character [11]. Moreover, the C(19)–C(20) (1.40(1) Å) and C(17)–C(18) (1.41(1) Å) bonds are significantly smaller than the other C C bonds (1.43(1) Å for C(18)–C(19), 1.46(1) Å for C(16)–C(17), 1.45(1) Å for C(16)–C(20)). Thus, the η^5-C_5H_4 ring shows fulvene character and the cation is illustrated as a resonance hybrid of the canonical structure of **A** and **B** (Scheme 2).

A projection of the unit cell along the *b* axis is shown in Fig. 3. The tetrahedral BF_4^- shows smaller thermal motion (B_{eq}, 4.7–9.7 $Å^2$) compared with the value of **3** (10.0–25.6 $Å^2$). The average F–B–F angle is 110(2)° and the average B–F distance is 1.35(3) Å; these values correspond well with those reported for the iodobiruthenocenium$^+$ BF_4^- salt [18]. The shortest intermolecular C ··· C distance (3.585(8) Å) is found in

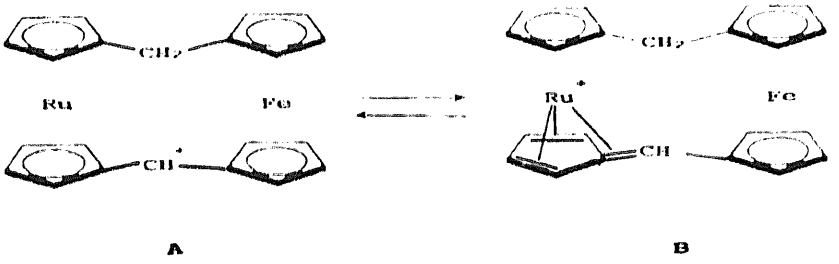

Scheme 2.

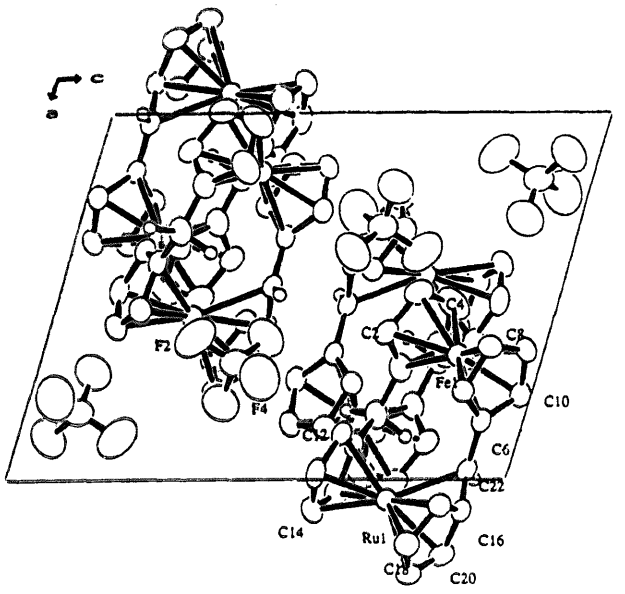

Fig. 3. Projection of the unit cell of **2** along *b* axis.

C(7) · · · C(21), which is longer than the sum of the van der Waals radii of two C atoms (3.40 Å). Therefore, there is absence of van der Waals contact between the cation–cation. The shortest distances between each F and C atoms in the cation are 3.313(7) Å for F(1)–C(22), 3.340(9) Å for F(2)–C(19), 3.229(7) Å for F(3)–C(13) and 3.196(9) Å for F(4)–C(14). Although all the values are somewhat larger than the sum of the van der Waals radii of F (1.35 Å) and C (1.70 Å) [11], the smaller BF_4^- anion sits near the higher positive charge of the

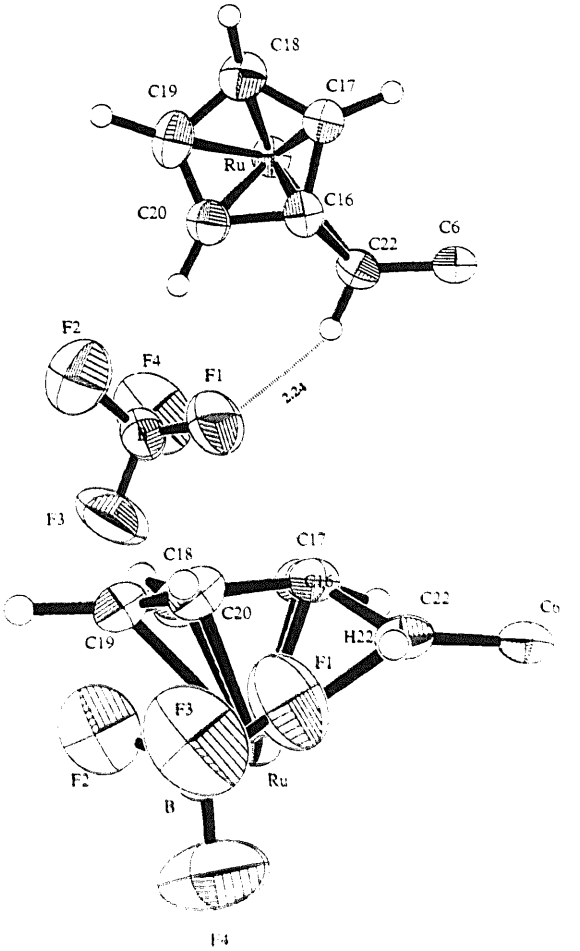

Fig. 4. ORTEP drawing of the $C_5H_4CH^+C$ and BF_4^-.

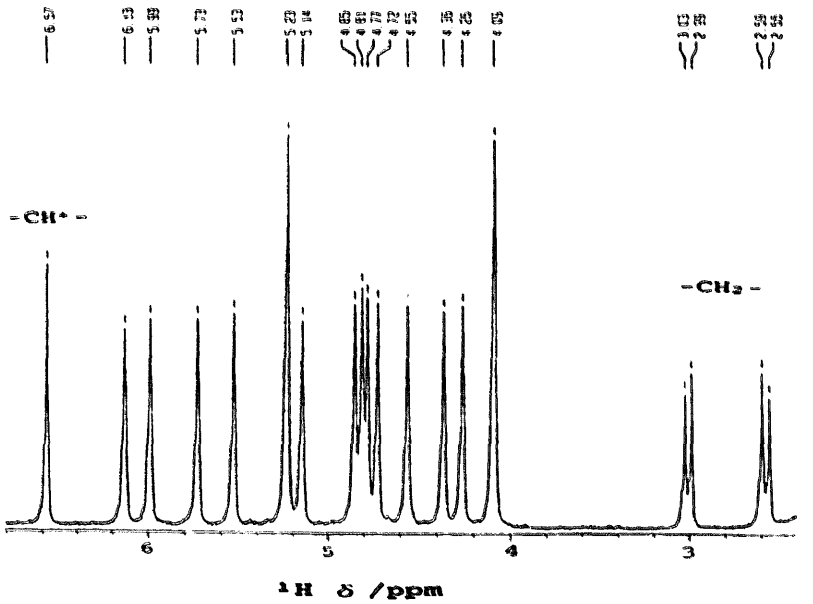

Fig. 5. ^1H NMR spectrum of **2** in CD_3CN.

Table 7
^{1}H NMR chemical shifts of 1 and 2

	Chemical shift δ	Assignment
1 [a]	3.44	$-CH_2-$
	4.08	$H_{2,5}$ (Fe moiety)
	4.21	$H_{3,4}$ (Fe moiety)
	4.51	$H_{2,5}$ (Ru moiety)
	4.68	$H_{3,4}$ (Ru moiety)
2 [b]	2.57, 3.01	H(21a, 21b)
	4.09	H(3, 4)
	4.26, 4.55	H(2.5)
	4.36, 4.72	H(7, 10)
	4.77, 4.81	H(8, 9)
	5.14, 5.53	H(12, 15)
	5.23	H(13, 14)
	4.85, 6.13	H(17, 20)
	5.73, 5.99	H(18, 19)
	6.57	H(22)
2 [c]	2.75, 3.09	H(21a, 21b)
	4.12, 4.22	H(3, 4)
	4.30, 4.63	H(2, 5)
	4.54, 4.87	H(7, 10)
	4.83	H(8,9)
	5.32, 5.70	H(12, 15)
	5.42, 5.44	H(13, 14)
	5.08, 6.35	H(17, 20)
	6.21, 5.96	H(18, 19)
	6.87	H(22)

[a] In $CdCl_3$; [b] in CD_3CN; [c] in CD_3COCD_3.

Ru site, especially the carbonium CH^+ center, as shown in Fig. 4. The distance between the F(1) and H(22) is found to be 2.40(4) Å, which is shorter the sum of the van der Waals radii of H (1.2 Å) and F (1.35 Å), suggesting the possibility of the hydrogen bond between them ($CH^+ \cdots F(1)BF_3$).

3.1. NMR studies

Salt 2 is easily soluble in polar organic solvents such as acetone and acetonitrile, giving a deep purple solution, whereas most ferrocenium cations give a green-blue solution. Fig. 5 shows the ^{1}H NMR spectrum of 2 in CD_3CN, and the chemical shifts are summarized in Table 7. Here, for the upper field, two signals at $\delta = 2.57$ (d $^2J_{21a,21b} = 20.0$ Hz) and 3.01 (d $^2J_{21b,21a} = 20.0$ Hz) are assigned as methylene (H(21a, 21b)); i.e. the methylene protons on the rigidly fixed C(21) are no longer equivalent and appear severally as a doublet. The lowest field signal at $\delta = 6.57$ can be assigned as H(22). This δ value is significantly smaller than the values reported for the α-carbonium analogous cations such as ferrocenylruthenocenylmethylium$^+$ cation ($\delta = 7.85$ at 183 K and 8.00 at 313 K [19]) and diruthenocenylmethylium$^+$ cation ($\delta = 7.72$ at 293 K [20]), probably because of a delocalization of the positive $-CH^+-$ charge perfectly over the Ru–CH^+ bond, whereas the positive charge is more localized in the $-CH^+-$ bond for the latter two carbonium salts.

The salt 2 gives 14 ring proton signals: the lower field seven signals at $\delta = 6.13$, 5.99, 5.73, 5.53, 5.23, 5.14 and 4.85 may be ascribed to the ring protons of the Rc moiety and the higher field seven signals at $\delta = 4.81$, 4.77, 4.72, 4.55, 4.36, 4.26 and 4.09 to those of the Fc moiety; i.e. the structure of the cation in solution remains intact in the solid. A similar ^{1}H NMR spectrum is given in 2 in CD_3COCD_3, although significantly lower field shifts are observed for all the signals (see Table 7); especially, the CH^+ (H(22)) signal shifts greatly ($\delta = 6.87$), probably because of the difference in dielectric constant of CD_3CN (ε 37.5) and CD_3COCD_3 (ε 20.7). Owing to the electrostatic interaction between the positive CH^+ charge and the higher dielectric constant solvent (CD_3CN), the positive CH^+ charge is decreased, giving higher field shifts.

To assign the other 14 signals, ^{1}H-NOSEY and COSY NMR spectroscopies were carried out in CD_3CN. From ^{1}H-NOSEY spectroscopy, the CH^+ signal (H(22), $\delta = 6.57$) correlates to the signal at $\delta = 6.13$ only. Firstly, it may be concluded that the peak at $\delta = 6.13$ is ascribed to the H(20), because the H(22) $\cdots$ H(20) distance (2.61 Å) is much shorter than the value of H(22) $\cdots$ H(17) (3.92 Å). From the ^{1}H-COSY spectroscopy, the number of correlation peaks at $\delta = 6.13$ is five (see Fig. 6), which means there is rapid syn–syn exchange motion, as in the case of neutral 1 [21]. Therefore, ring H atoms in the 2- and 5-positions are equivalent; thus the peak at $\delta = 6.13$ is ascribed to H(20) and H(17). Other signals are assigned using the same technique and the results are summarized in Table 7.

As the carbon signal of $-CH^+-$ is superimposed on the large CN signal in CD_3CN near $\delta = 120$, ^{13}C NMR and DEPT NMR spectra of 2 are measured in CD_3COCD_3, and the spectra and δ values are shown in Fig. 7 and Table 8; 17 strong intensity signals and five weak signals ($\delta = 120.91$, 119.53, 99.87, 91.43 and 80.09) are observed. To assign the two weak signals at lower field ($\delta = 120.91$ and 119.53), ^{13}C-DEPT NMR spectroscopy of 2 was carried out. The four nonhydrogen carbon atoms (C_1) observed at $\delta = 120.91$, 99.87, 91.43 and 80.09 disappear; the former two signals can be assigned as C_1 for the Rc moiety ($\delta = 120.91$ assigned as C(16), 99.87 C(11)) and the latter two as being for the Fc moiety ($\delta = 91.43$ C(6), 80.09 C(1)). The lower field signal at $\delta = 119.53$ is ascribed to $-CH^+-$ (C(22)) and the higher field signal at $\delta = 22.98$ is ascribed to $-CH_2-$ (C(21)). The former δ value corresponds well to the value reported for analogous salts, such as ferrocenylruthenocenylmethylium cation ($\delta = 111.3$ and 117.8 at 183 and 323 K respectively) [19], diruthenocenylmethylium cation ($\delta = 111.8$) [20], $FcCH_2^+$ (Fc; $Cp(C_5H_4)Fe$, $\delta = 117.3$) and $FcCH^+Ph$

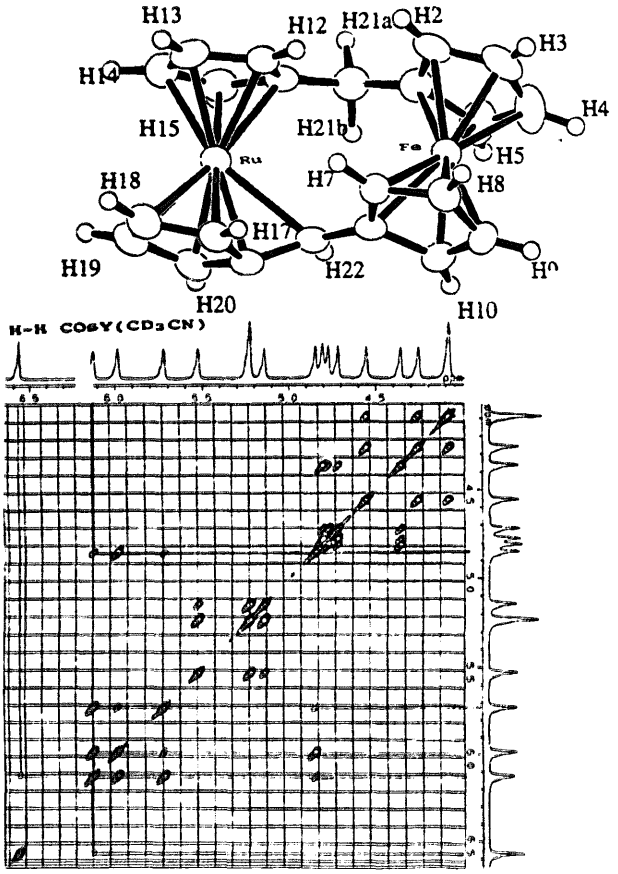

Fig. 6. ^{1}H-COSY NMR spectrum of **2** in CD_3CN.

($\delta = 121.5$) [22]. However, all measurements of the ^1H–^{13}C shift correlation of the 2D NMR spectra to assign the other 16 signals have been unsuccessful because of the instability in CD_3COCD_3 during measurements (3–4 days); the lower field eight lines are ascribed to the ring protons of the Rc moiety and other eight lines to the Fc moiety.

Fig. 8 shows ^{13}C CP/MAS NMR spectra of **1** (a) and single crystal salt **2** (b). As has been mentioned previously, **1** gives four signals ($\delta = 69.27$, 71.98, 88.11 and 27.21) [1]. The lower field signal at $\delta = 88.11$ is assigned as the C_1 atoms, i.e. the C_1 signals of the Rc and Fc moieties are not well-resolved, there being only slight chemical shift differences between them. The signals at $\delta = 71.98$ and 69.27 are assigned as Cp-ring carbons (CH) of the Rc and Fc moieties respectively, and the $-CH_2-$ signal is observed at $\delta = 27.21$. In contrast to the sharp signals of **1**, several broader signals are observed for **2** because the chemical shift spreads out extensively, as shown in the ^{13}C NMR spectra in CD_3COCD_3.

On the basis of ^{13}C NMR spectra of **2** in CD_3COCD_3, the higher field signal at $\delta = 24.58$ is ascribed to the $-CH_2-$ (C(21)), which shows an upfield shift (2.63 ppm), as in the case of **3** compared with the value of **1**. The strong intensity signals are ascribed to the ring C atoms in the Fc ($\delta = 71.98$) and Rc ($\delta = 80.63$, 86.65^{sh}) moieties. Although a small lower field shift ($\Delta\delta = 2.71$)

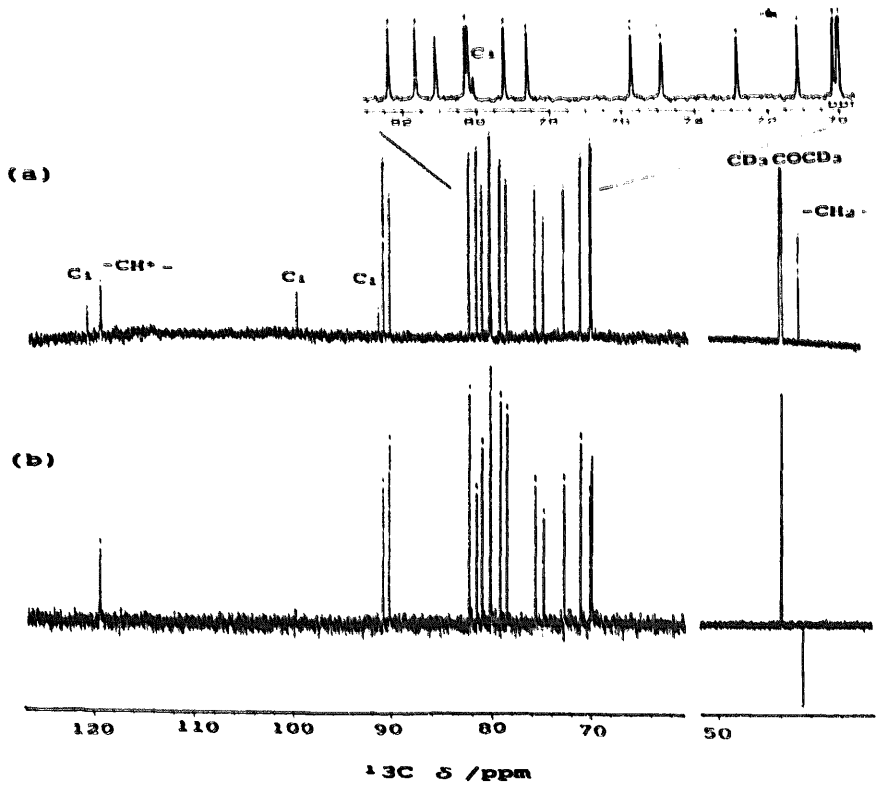

Fig. 7. ^{13}C NMR spectra of **2** in CD_3COCD_3.

Table 8
^{13}C NMR chemical shifts of 1 and 2

	Chemical shift δ	Assignment
1 [a]	90.07	C_1 (Ru moiety)
	86.83	C_1 (Fe moiety)
	72.33, 69.34	(Ru moiety)
	69.05, 67.05	(Fe moiety)
	26.83	$-CH_2-$
2 [b]	– [d]	
	99.95 – [d]	C_1 (Ru moiety)
	90.84, 90.30	(Ru moiety)
	82.45, 81.81	(Ru moiety)
	81.13, 80.24	(Ru moiety)
	80.20, 79.40	(Ru moiety)
	91.24, 79.94	C_1 (Fe moiety)
	78.54, 75.87	(Fe moiety)
	74.94, 72.90	(Fe moiety)
	71.35, 70.31	(Fe moiety)
	70.18, 70.14	(Fe moiety)
	23.15	$-CH_2-$
2 [c]	119.53	$-CH^+-$
	120.91, 99.87	C_1 (Ru moiety)
	90.88, 90.27	(Ru moiety)
	82.38, 81.64	(Ru moiety)
	81.09, 80.28	(Ru moiety)
	80.21, 79.22	(Ru moiety)
	91.43, 80.09	C_1 (Fe moiety)
	78.59, 75.71	(Fe moiety)
	74.88, 72.83	(Fe moiety)
	71.16, 70.15	(Fe moiety)
	70.04, 69.99	(Fe moiety)
	22.98	$-CH_2-$

[a] In $CDCl_3$; [b] in CD_3CN; [c] in CD_3COCD_3. [d] The $-CH^+$ and the other C_1 signal δ values could not be estimated owing to the overlapping of the solvent (CD_3CN; δ 120 (CN)) signal.

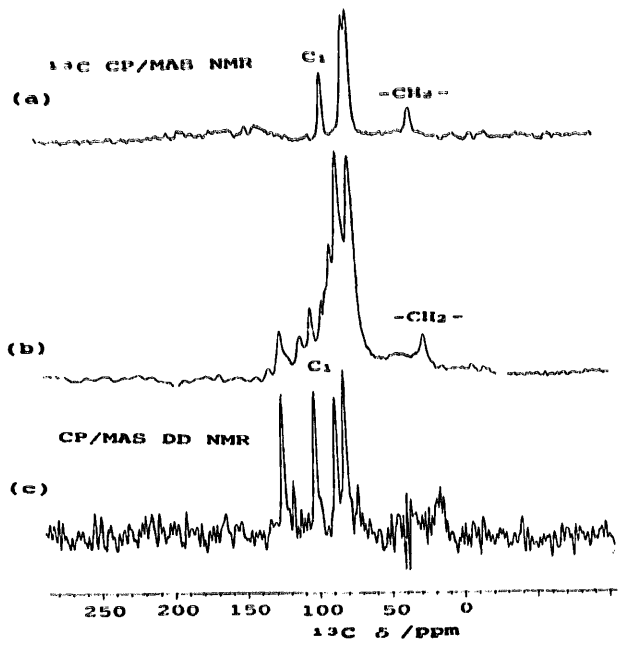

Fig. 8. ^{13}C CP/MAS NMR spectra of 1 (a), 2 (b) and its DD NMR spectra of 2 (c).

is observed for the Fc moiety, larger shifts ($\Delta\delta = 8.7$–14.7) are found in the Rc moiety because of Ru–CH^+ bond formation. The DD technique was applied to detect the C_1 signals. With increasing delay times for decoupling and data acquisition, the signals of CH- and CH_2-type decayed rapidly, and the four C_1 signals were observed clearly. On the basis of ^{13}C NMR spectra in solution, the higher field two signals at $\delta = 86.65$ and 80.24 are ascribed as C_1 signals for the Fe side (C(1) and C(6) respectively) and the lower field signals at $\delta = 101.12$ and 123.27 are for the Ru side (C(11), C(16) respectively). The signal at $\delta = 108.70$ is ascribed as $-CH^+-$ (C(22)), although a smaller higher field shift is observed compared with the value in CD_3COCD_3 ($\delta = 119.53$).

4. Conclusion

From the results obtained in the present studies, it can be concluded that compound 1 reacts with $[RcHCl]^+BF_4^-$ and $[RcHBr]^+BF_4^-$ giving a monocationic salt 2. The cation is shown as a resonance hybrid canonical structure of η^6-fulvalene formulated as $[Fe^{II}(C_5H_4CH_2C_5H_4)(C_5H_4CH{=}C_5H_4)Ru]^+$ and α,α-carbonium type formulated as $[Fe^{II}(C_5H_4CH_2C_5H_4)(C_5H_4CHC_5H_4)Ru]^+$ with Ru–C_α covalent bond. The positive $-CH^+-$ charge is delocalized over the bond, resulting in the stability of the α,α-carbonium salt. In contrast, 1 reacts with $[RcHI]^+BF_4^-$ giving a monocationic salt 3 expressed as $[Fe^{II}(C_5H_4CH_2C_5H_4)_2Ru^{IV}I]^+BF_4^-$ with a stable Ru^{IV}–I bond, as shown in Scheme 1. A similar conclusion has reported by the present authors; i.e. ferrocenylruthenocenylmethane and diruthenocenylmethane react with $[RcHCl]^+BF_4^-$ and $[RcHBr]^+BF_4^-$ giving their α,α-carbonium salts and with $[RcHI]^+BF_4^-$ giving their iodoruthenocenium salts [19,20]. As mentioned in previous reports, the stability of the Ru^{IV}–X (X = Cl, Br, I) bond in the $[RcHX]^+$ cation increases in the order Cl < Br < I. Thus, the stability of Ru^{IV}–I prevents the formation of the α,α-carbonium salt by using $[RcHI]^+BF_4^-$. Owing to the lesser stability of Ru^{IV}–Cl and Ru^{IV}–Br, the $-CH_2-$ in 1 was oxidized predominantly giving a carbonium cation 2 by using $[RcHX]^+BF_4^-$ (X = Br, Cl).

References

[1] M. Watanabe, I. Motoyama, T. Takayama, M. Shimoi and H. Sano, *J. Organomet. Chem.*, *496* (1995) 87.
[2] A.F. Diaz, U.T. Muller-Westehoff, A. Nazzal and M. Tanner, *J. Organomet. Chem.*, *236* (1982) C45.
[3] M. Watanabe and H. Sano, *Bull. Chem. Soc. Jpn.*, *63* (1990) 777.
[4] A. Bax, *Two-Dimensional Nuclear Magnetic Resonance in Liquids*, Reidel, Boston, 1982.

[5] D.T. Cromer and J.T. Waber, *International Tables for X-Ray Crystallography*, Vol. IV, Kynoch Press, Birmingham, UK, 1974, Table 2.2A.
[6] J.A. Ibers and W.C. Hamilton, *Acta Crystallogr., 17* (1964) 781.
[7] D.C. Creagh and W.J. McAuley, *International Tables for X-Ray Crystallography*, Vol. C, Kluwer Academic, Boston, 1992, Table 4.2.6.8, pp. 219–222.
[8] TEXSAN: *Crystal Structure Analysis Package*, Molecular Structure Corporation, 1985.
[9] A.L. Rheingold, U.T. Muller-Westerhoff, G.F. Swiegers and T.J. Haas, *Organometallics, 11* (1992) 3411.
[10] A.Z. Kreindlin, P.U. Petrovskii, M.I. Rybinskaya, A.I. Yanovskii and Y.T. Struchkov, *J. Organomet. Chem., 319* (1987) 229.
[11] L. Pauling, *The Nature of the Chemical Bond*, Cornell University Press, 3rd ed., 1960.
[12] A.A. Koridze, N.M. Astakhova and P.V. Petrovskii, *J. Organomet. Chem., 254* (1983) 345.
[13] M.I. Rybinskaya, A.Z. Kreindlin, Y.T. Struchkov and A.I. Yanovsky, *J. Organomet. Chem., 359* (1989) 233; A.I. Yanovsky, Y.T. Struchkov, A.Z. Kreindlin and M.I. Rybinskaya, *J. Organomet. Chem., 369* (1989) 125.
[14] S. Lupan, M. Kapon, M. Cais and F.H. Herbstein, *Angew. Chem., 84* (1972) 1104.
[15] U. Behrens, *J. Organomet. Chem., 182* (1979) 89.
[16] T.D. Turbitt and W.E. Watts, *J. Chem. Soc. Perkin II*, (1974) 1974.
[17] A.M. Eastoz, M.J.A. Habib, J. Park and W.E. Watts, J. Chem. Soc. Perkin II, (1972) 2290.
[18] M. Watanabe, I. Motoyama, M. Shimoi and T. Iwamoto, *Inorg. Chem., 33* (1994) 2518.
[19] M. Watanabe, T. Iwamoto, S. Nakashima, H. Sakai and I. Motoyama, *J. Organomet. Chem., 448* (1993) 167.
[20] M. Watanabe, I. Motoyama and H. Sano, *Inorg. Chim. Acta, 225* (1994) 103.
[21] U.T. Muller-Westerhoff *Angew Chem. Int. Ed. Engl., 25* (1986) 702; A. Cassens, P. Elbracht, A. Nazzal, W. Prossdorf and U.T. Muller-Westerhoff, *J. Am. Chem. Soc., 103* (1981) 6367.
[22] A.A. Koridze, N.M. Astakhova and P.V. Petrosvskii, *J. Organomet. Chem., 254* (1983) 345.